RSC Advances

PAPER

View Article Online
View Journal | View Issue

Cite this: *RSC Adv.*, 2018, **8**, 11991

Highly sensitive and wearable gas sensors consisting of chemically functionalized graphene oxide assembled on cotton yarn†

Min-A. Kang,[abc] Seulgi Ji,[a] Seongjun Kim,[a] Chong-Yun Park,[c] Sung Myung,*[a] Wooseok Song,[a] Sun Sook Lee,*[a] Jongsun Lim[a] and Ki-Seok An[a]

Received 7th February 2018
Accepted 20th March 2018

DOI: 10.1039/c8ra01184b

rsc.li/rsc-advances

Highly sensitive and wearable chemical sensors for the detection of toxic gas molecules are given significant attention for a variety of applications in human health care and environmental safety. Herein, we demonstrated fiber-type gas sensors based on graphene oxide functionalized with organic molecules such as heptafluorobutylamine (HFBA), 1-(2-methoxyphenyl)piperazine (MPP), and 4-(2-keto-1-benzimidazolinyl)piperidine (KBIP) by assembling functionalized graphene oxide (FGO) on a single yarn fabric. These gas sensors of FGO on yarn exhibited extraordinarily higher sensitivity upon exposure to gas molecules than chemically reduced graphene oxide due to many active functional groups on the GO surface. Furthermore, the mechanical stability and chemical durability of the resulting gas sensors are well-maintained. Based on these results, we expected that our sensors with high sensitive and wearability will provide a good premise for wearable chemical sensors-based multidisciplinary applications.

Introduction

Gas sensors that provide information regarding the presence and concentration of specific gas molecules in the ambient atmosphere have been used for human health,[1] indoor and outdoor environmental monitoring,[2,3] and medical diagnostics.[4] Among various types of gas sensors, commercially available metal-oxide-based gas sensors have been investigated for several years owing to their relatively low cost and high sensitivity, but typical metal-oxide-based gas sensors require high operating temperatures of at least 200 °C for effective interaction with the target gas.[5–7] Owing to the resulting high power consumption and difficulty in obtaining a ppb (parts per billion)-level sensitivity, there is a limitation in their application to flexible and stretchable fabric-based highly sensitive sensors. Recently, to overcome this limitation, graphene-based materials have been utilized for the fabrication of micrometer-sized gas sensors, in which the adsorbed gas molecules contributed to step-like resistance change of graphene with a massless Dirac fermion by effectively controlling the local carrier concentration.[8,9] These graphene-based devices have high sensitivity down to ppb levels even at room temperature and outstanding resistance change depending on gas adsorption owing to their sensitive electrical interaction with gas molecules.[10–12] Moreover, graphene-based gas sensors have relatively short response and recovery times because the gas molecules are bonded to weak-bonding, which directly affects the electrical properties of graphene. However, intrinsic graphene does not have a functional group, which is a site where specific gas molecules can be adsorbed onto the surface. To overcome these limitations, many studies have been carried out to hybridize graphene with gas-sensitive metal (or metal oxide) nanoparticles (NPs),[13–16] exploit mesh-type substrates for the improvement of surface area,[17,18] and utilize reduced graphene oxide (rGO) with functional groups and defects for the enhancement of sensing performance.[19,20] In the case of metal (or metal oxide) NPs acting as catalysts, the speed of detection is very fast, but high operating temperature is required to obtain excellent sensitivity. Furthermore, a complicated annealing process is required to hybridize metal (or metal oxide) NPs with graphene.[16] In the case of rGO with active sites, it is possible to manufacture flexible sensors and employ them in body-attachable and wearable devices owing to their inherent flexible properties. Functionalization processes of graphene surface are still required for the sensitive sensing of specific gas molecules.

In our study, we successfully developed highly sensitive and wearable gas sensors on fabric substrates by using functionalized graphene oxide (FGO), which has higher gas adsorption sensitivity than pristine graphene. First, FGO was functionalized with three kinds of organic molecules *i.e.*, 2,2,3,3,4,5,5-

[a]*Thin Film Materials Research Center, Korea Research Institute of Chemical Technology, Daejeon 305-600, Republic of Korea. E-mail: msung@krict.re.kr; sunsukl@krict.re.kr*

[b]*Department of Energy Science, Sungkyunkwan University, Suwon, Gyeonggi-do 440-746, Republic of Korea*

[c]*Department of Physics, Sungkyunkwan University, Suwon, Gyeonggi-do 440-746, Republic of Korea*

† Electronic supplementary information (ESI) available. See DOI: 10.1039/c8ra01184b

heptafluorobutylamine (HFBA) with amine groups, 1-(2-methoxyphenyl)piperazine (MPP), and 4-(2-keto-1-benzimidazolinyl)-piperidine (KBIP). FGOs with specific functional groups have distinct sensing characteristics owing to the different number of lone pair of electrons, and these functional groups are sites where reactions with specific gas molecules occur easily. Finally, a wearable gas sensor with significantly enhanced gas response was demonstrated by using FGO.

Results and discussion

First, GO obtained using the modified Hummers' method was functionalized with specific chemical molecules for the fabrication of fiber-type flexible devices based on FGO on a single yarn (Fig. 1).[21,22] HFBA, MPP, and KBIP were used as chemical agents for the modification of the GO surface by using a method similar to that used in our previous study.[23] The well-known nucleophilic substitution reaction of the epoxy groups on the GO surface was utilized for the functionalization of GO nanosheets. When HFBA was used as the precursor in the functionalization reaction, the lone pair of electrons of the amine group in HFBA breaks one of the C–O bonds in the GO sheets. Subsequently, the lone pair of electrons from oxygen breaks the N–H bond, which results in an alcohol group as the oxygen forms a bond with hydrogen from the broken N–H bond. When MPP and KBIP are used, highly diverse FGOs with different terminal groups can be synthesized *via* the same method. FGO nanosheets were dispersed in dimethylformamide with ultrasonic vibration for 20 min to prepare an FGO suspension. For the assembly of FGO on the yarn surface, commercially available yarn was placed in the FGO suspension for 30 min, and thereafter rinsed thoroughly with distilled water four times.

Scanning electron microscope (SEM) analysis was utilized to characterize the microstructure of the FGO (GO) nanosheets on yarn surfaces. Fig. 1(b) shows the SEM images of single yarn coated with FGO synthesized using HFBA, MPP, and KBIP as the chemical ligands of the GO nanosheets. As shown in the SEM images, FGO nanosheets were uniformly coated on the yarn surface. These FGO nanosheets had stable structures on the yarn after rinsing with water, and hence, we could perform additional processing steps for the fabrication of fiber-type devices (Fig. S1 in ESI†). Furthermore, the contact angle was measured by coating rGO or FGO on a cotton fabric using the same dipping process (Fig. S2 in ESI†). Water droplets were easily absorbed when pure cotton fabric and cotton fabric were coated with graphene oxide, whereas rGO- and FGO-coated fabrics exhibited a relatively hydrophobic surface.[24] This result indicates that single yarn, an element of cotton fabric, is also uniformly coated on the surface with rGO (or FGO) over the entire area.

X-ray photoelectron spectroscopy (XPS) was used to analyze the atomic compositions and stoichiometric ratios of GO, rGO, and FGO assembled on the yarn surface. XPS spectra were recorded using a monochromatic Al kα ($h\nu = 1486.6$ eV) source and normal emission geometry. Fig. 2(a) shows the XPS spectra of GO, rGO, and FGO nanosheets assembled on a yarn surface. The C1s core level spectra were deconvoluted using the Voigt function.[25] Four C1s peaks of GO nanosheets on yarn fiber at 284.5, 285.3, 288.4, and 289.2 eV were observed, which were assigned to C–C, C–O, C═O, and O–C═O, respectively.[26] For rGO and FGO modified with KBIP, MPP, and HFBA, the intensity of the oxygenated groups in the C1s peak decreased significantly, and oxygen-containing groups were eliminated during the reduction and functionalization processes. The C/O ratio of GO, rGO reduced by hydrazine, and FGO with KBIP, MPP, and HFBA were 0.45, 5.07, 5.32, 4.62, and 5.2, respectively. This result also confirms the significant reduction of GO after its functionalization process. It is advantageous that the application of the functionalization process enhances the conductivity of the nanosheets, and our FGO nanosheets are readily applicable as electrodes or channel materials in device applications. In the case of HFBA-FGO on yarn fiber, the peak associated with F1s was also observed, indicating that GO was successfully functionalized (Fig. 2(b)-(vi)). The structural characterizations of GO, rGO, KBIP-GO-Y, MPP-GO-Y, and HFBA-GO-Y were performed using resonant Raman spectroscopy. All the Raman spectra were recorded at an excitation wavelength of 514 nm under ambient conditions. Fig. 2(b) shows the Raman spectra of only GO, rGO reduced by hydrazine, FGO with KBIP, MPP, and HFBA on the yarn fiber, in which the Raman fingerprints of GO, including the D-band (~1355 cm^{-1}) and G-band

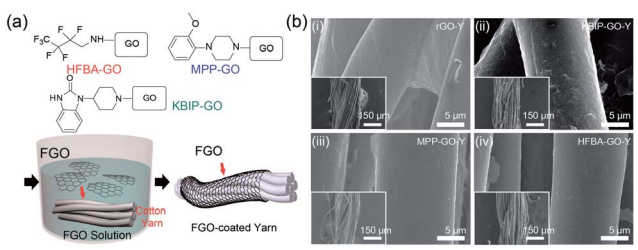

Fig. 1 (a) Schematic diagram of functionalized graphene oxide (FGO) coated on single yarn for gas detection. (b) SEM images of (i) rGO, (ii) KBIP-GO, (iii) MPP-GO, and (iv) HFBA-GO coated on single yarn.

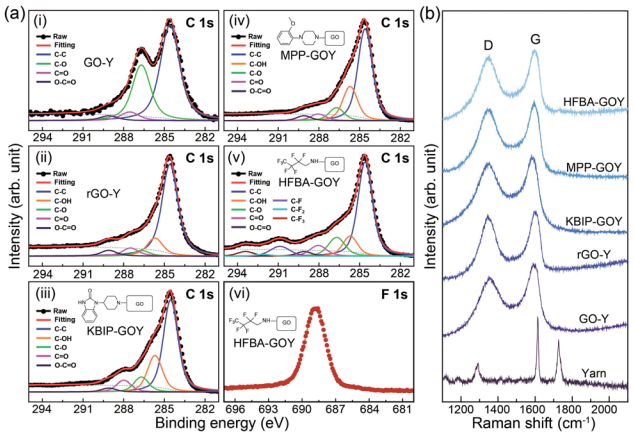

Fig. 2 (a) The C1s peak in the XPS spectra of (i) GO and (ii) rGO nanosheets coated on yarn, FGO nanosheets functionalized with (iii) KBIP, (iv) MPP, and (v) HFBA agents. (vi) The F1s peaks of HFBA-GO on yarn. (b) Raman spectra of GO, rGO, and FGO on yarn and only yarn fibers.

(~1591 cm^{-1}), are apparent. The Raman spectrum of rGO reduced by hydrazine on the yarn had a D-band at 1345 cm^{-1} and G-band at 1602 cm^{-1}. In the case of FGO modified with KBIP, MPP, and HFBA on the yarn fiber, a D-band at 1350 cm^{-1} and G-band at 1590 cm^{-1} were also observed.[26,27] The G-band of FGO with KBIP, MPP, and HFBA on the yarn fiber exhibited a significant redshift, similar to that of rGO reduced by hydrazine. This result indicates that our functionalization is a promising reducing method and does not require highly toxic agents such as hydrazine.

Recently, there have been many studies about the detection of gases such as NH_3, NO_2, and fine dust with high performance to prevent environmental pollution.[28,29] It is also necessary to monitor pollutants emitted by industrial or recycling processes. FGO nanosheets on yarn fibers were used to improve the electrical response of the exposure to specific gases (Fig. 3(a)). Upon investigation of the gas response to NO_2 or NH_3 using only carbon tape as a channel, remarkable changes could not be observed (Fig. S3 in the ESI†). This result suggests that carbon tape used as an electrode did not show any sensitivity to gas injection. Herein, the length and width of the FGO-based sensors were approximately 540 and 470 μm, respectively, when carbon tape was used as the electrode. Furthermore, tape adhesion test which is a simple and easily practical method for confirming the degree of adhesion of the FGO was also performed using carbon conductive double-faced adhesive tape (Nisshin EM Co., Ltd.) in Fig. S4 in the ESI.† The surface morphology and the resistance value of FGO-based devices does not change dramatically. This result showed the superior mechanical adhesion of FGO deposited on the single yarn. The electrical resistance of the sensors was monitored under a bias voltage of 0.1 V. Fig. 3(b) shows the gas sensing response of rGO and FGO nanosheets on yarn fibers to NH_3 and NO_2 molecules at room temperature. The gas sensitivity was calculated using $\Delta R/R_{N_2} = (R_{gas} - R_{N_2})/R_{N_2}$, where R_{gas} and R_{N_2} represent the resistances of the device to specific gases and N_2 gas, respectively. NH_3 and NO_2 molecules absorbed on the rGO and FGO surfaces acted as the electron donor and acceptor, respectively.[30] The electrical resistance change of the gas sensor based on FGO nanosheets with KBIP, MPP, and HFBA on the yarn fiber to NH_3 exposure was approximately three times higher than that based on rGO nanosheets. The electrical resistance of FGO with KBIP increased by 70%, whereas rGO-based sensors exhibited an electrical resistance change of only 12% under exposure to 8 ppm NH_3. In the case of NH_3 gas, the minimum concentration of 0.5 ppm and gas response with positive sensitivity were observed. In the case of NO_2 gas with 1.5 ppm concentration, gas response with negative sensitivity was observed, and the gas response was proportional to the gas concentration. Under 3 ppm NO_2 exposure, the electrical resistances of FGO with KBIP and rGO decreased by 65% and 25%, respectively. Notably, KBIP-GO-Y showed the best gas response to NO_2 and NH_3 gas. This phenomenon can be explained by the presence of the lone pair of electrons. KBIP-GO-Y, MPP-GO-Y, and HFBA-GO-Y have 4, 3, and 1 adsorbing sites, respectively, and the gas response of KBIP-GO-Y was higher than those of MPP-GO-Y, HFBA-GO-Y, and rGO-Y. Furthermore, the gas response of the fabric-based gas sensors increased twice under 0.15 ppm NO_2 exposure, when compared to that of the yarn-based gas sensor (Fig. S5†). This is because fabric-based devices have large surface area where gas molecules can be adsorbed.

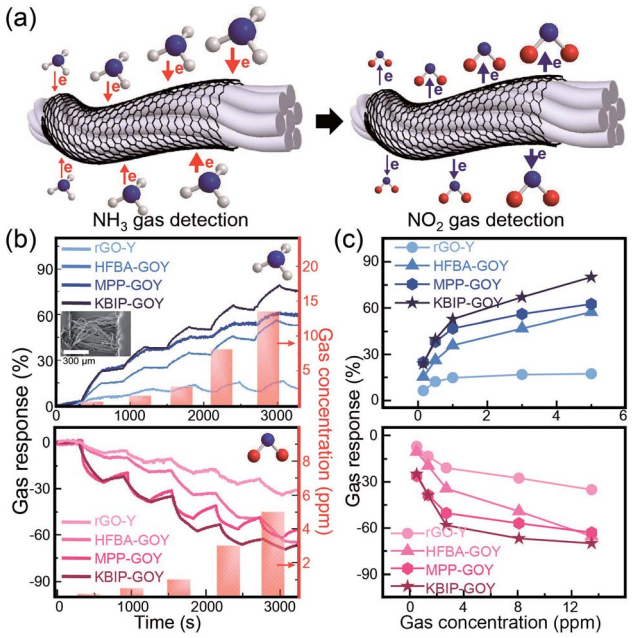

Fig. 3 (a) Schematic illustration of yarn-fabric-based gas sensor assembled with FGO. (b) Real-time gas sensing response to NH_3 (top) and NO_2 (bottom) molecules at room temperature under various exposure conditions. (c) Gas response of rGO and FGO on yarn fiber to NH_3 (top) and NO_2 (bottom) molecules as a function of gas concentration.

The gas response of thin-film-type FGO-based devices was also investigated under exposure to NO_2 and NH_3. Thin-film-type devices were prepared by spin coating the GO and FGO solutions onto SiO_2 substrate to further clarify the effects of the functional groups (Fig. S6 in the ESI†). The gas sensor based on the thin film exhibited a similar tendency as the gas sensor based on a single yarn, revealing that the functional groups bonded with GO had a strong influence on the gas response.

Flexibility is a key factor in wearable and body-attachable devices. The evaluation of the durability of electrical resistance and the sensing performance of gas sensors based on FGO and rGO nanosheets is shown in Fig. 4. A bending tester (JUNIL TECH Co., LTD-JIBT-610 (Radius Bending)) was used, and the fiber-type sensors were bent down to a bending radius of 0.2 mm (Fig. 4(a)). As shown in Fig. 4(b), the resistance of all the fiber-type FGO- and rGO-based sensors was still stable after 10^4 bending cycles. This electrical stability of the FGO- and rGO-based sensors in the bending test was presumably due to the superior mechanical flexibility of GO.[31] Further, the resistance changes increased slightly after 10^4 bending cycles. However, this value was less than 5%, indicating that there was no significant difficulty in their application to wearable devices. The inset shows a yarn-based flexible device sewed in different letters on a woven fabric, which is applicable to flexible electronics. We confirmed the resistance by connecting the wire to

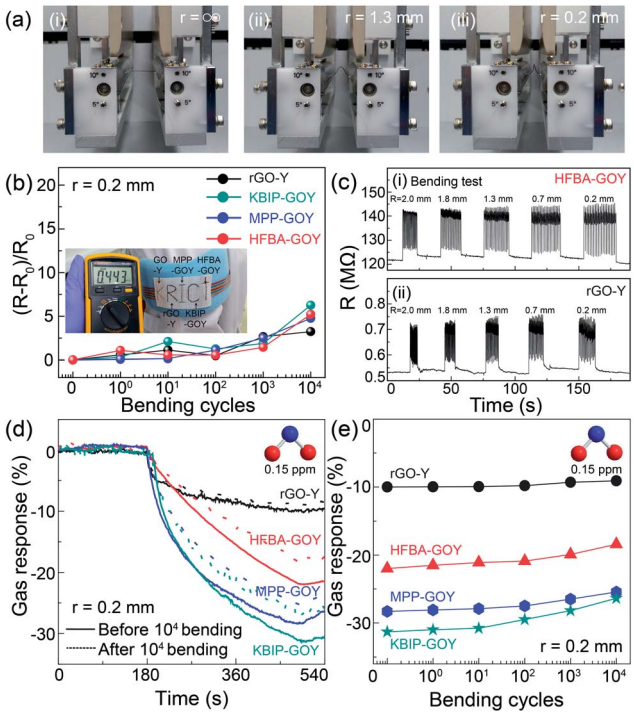

Fig. 4 Evaluation of the durability and performance of FGO- and rGO-based sensors for monitoring the resistance variation under exposure to NO_2. (a) Bending test of gas sensors based on FGO and rGO nanosheets on yarn fiber. (b) The resistance variation of fiber-type sensors based on FGO and rGO according to the number of bending cycles (bending radius = 0.2 mm). The inset image is a yarn-based device sewed in different letters on a woven fabric. (c) Real-time monitoring of resistance of sensors based on FGO with HFBA and rGO during the bending test under various bending conditions. (d) Time-dependent electrical response of gas sensors based on FGO and rGO nanosheets after 10^4 cycles of bending test under exposure to 0.15 ppm NO_2 at the bias voltage (V_{DS}) = 0.1 V. (e) Gas response of FGO- and rGO-based gas sensors as a function of the number of bending cycles (bending radius = 0.2 mm).

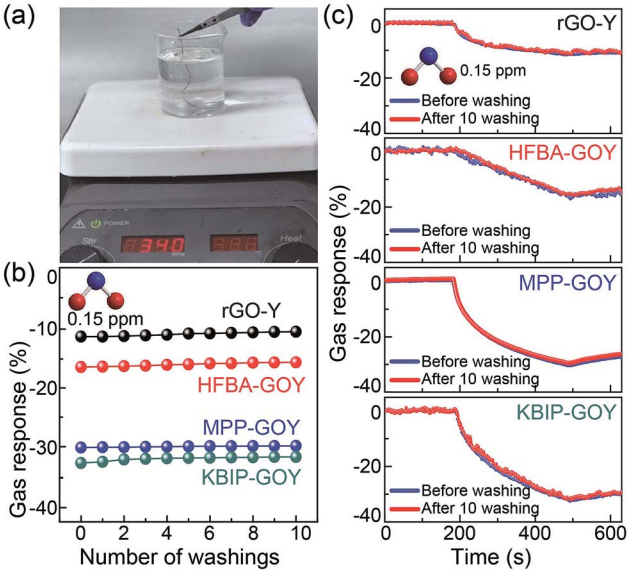

Fig. 5 (a) Photograph of the washing process using FGO-based yarn. (b) Gas response depending on the number of washing cycles under exposure to 0.15 ppm NO_2 gas. (c) Gas response of rGO-Y, HFBA-GO-Y, MPP-GO-Y, and KBIP-GO-Y before and after washing for 10 times.

the yarn fiber on the back of the woven fabric. Fig. 4(c) shows the mechanical stability test of HFBA-GO-Y with the best gas response and that of rGO-Y by measuring the resistance change depending on the bending radius. The device performance was evaluated at the bending radii of 0.2, 0.7, 1.3, 1.8, and 2.0 mm, and consequently, the resistance change was observed to be almost constant for different bending radii. The outstanding stability and flexibility demonstrated herein render the flexible fabric-based devices suitable for wearable and body-attachable applications. We also monitored the resistance of the sensors in real time under various gas exposure conditions after 10^4 bending cycles. The FGO- and rGO-based sensors exhibited low reduction in NO_2 sensing after 10^4 bending cycles. For instance, the gas response of the sensors based on FGO nanosheets with KBIP, MPP, and HFBA and rGO was reduced after 10^4 bending cycles by 27%, 25%, 18%, and 10%, respectively (Fig. 4(d)). This result does not indicate a large degradation in consideration of the number of bending cycles. Fig. 4(e) shows the gas response depending on the number of bending cycles. As shown in the figure, bending cycles up to 10^3 were stable to a certain degree with no significant reduction. Thereafter, a slight degradation was identified for bending cycles up to 10^4. These results indicate that the poor adhesion between the carbon electrode and FGO and rGO channels was caused by the bending process. Nevertheless, the deterioration was not remarkable as compared with that in the previous report.[32]

Washing durability, an important parameter of wearable electronic devices, is essential to confirm whether the electrical properties are maintained in water or chemical detergents. In order to demonstrate the durability, we soaked rGO-Y, KBP-GO-Y, MPP-GO-Y, and HFBA-GO-Y in a beaker containing deionized water and stirred at 340 rpm for 30 min (Fig. 5(a)). Notably, the gas response changes according to the number of washing times were negligible under exposure to 1.5 ppm NO_2 gas (Fig. 5(b)). Furthermore, Fig. 5(c) shows the gas response before and after washing for 10 times. In the above plot (Fig. 5(c)), the gas response changed negligibly and the output curve showed only slight changes (Fig. S7†). For industrial applications, laundry test was also carried out using commercial synthetic detergents (Power Clean Total Care, Korea) (Fig. S8 in ESI†).[33] This result demonstrates that the FGO nanosheets on yarn fibers are chemically inert and are preserved without significant damage.

Conclusions

In summary, we successfully fabricated FGO-based gas sensors on yarn fibers using HFBA, MPP, and KBIP-GO. FGO-based gas sensors were produced by using a simple dipping process. The sensors with KBIP-GO-Y showed extremely high sensitivity (~70%) for exposure to gas molecules compared with rGO-based sensors (~12%) in spite of relatively low gas concentrations (8 ppm NH_3 gas). When exposed to 3 ppm NO_2 gas, the gas sensors composed of KBIP-GO-Y and rGO-Y achieved gas

responses of 65% and 25%, respectively. Moreover, the mechanical stability of the fabricated sensors was outstanding after 10^4 bending cycles and the chemical durability was constant even after washing for 10 times with deionized water. Our yarn-fiber-based gas sensors are promising devices for highly sensitive wearable and body-attachable sensor applications.

Experimental

Synthesis of GO with functional groups

GO was synthesized from commercially available graphene using the modified Hummers' method.[21,22] First, graphene flakes (Sigma-Aldrich) were oxidized by using $NaNO_3$, H_2SO_4, $KMnO_4$, and H_2O_2. The obtained GO was repeatedly washed *via* centrifugation to remove large GO, and the product was dispersed in deionized water. Accordingly, the as-prepared GO sheet was exfoliated using ultrasonic treatment and the solvent was evaporated to attain solid crumbs of the GO sheet. Subsequently, the GO sheets synthesized in the reaction flask (100 mg) and KBIP (362 mg, 1.82 mmol) were mixed with 3 mL of dimethylacetamide. The mixture was stirred overnight at 100 °C, thereafter cooled down to room temperature, and repeatedly filtered with three solvents (methylene chloride, chloroform, and methanol) by utilizing polytetrafluoroethylene membrane as the filter paper. Consequently, it was dried in a vacuum oven at 80 °C to obtain GO functionalized with KBIP. Three functionalized GO samples with diverse functional groups were synthesized using the above method.

Assembly of FGO and rGO nanosheets on the cotton yarn and fabric surface

A simple dipping process was employed for the formation of FGO single yarn and fabric. First, single yarn and fabric were rinsed carefully with distilled water to remove dust or impurities on the surface. Subsequently, commercially available cotton yarn and fabric were placed in the FGO suspension for 30 min and thereafter dried in a vacuum oven at 80 °C. Finally, the FGO yarn and fabric were rinsed thoroughly with distilled water for four times to prevent the formation of FGO agglomerations. In the case of rGO, the same process was applied with a GO suspension. Subsequently, GO single yarn and fabric were chemically reduced with hydrazine in a vacuum oven at 80 °C for 15 h.

Gas sensing measurement of the FGO- and rGO-based devices

In order to measure the gas response of the FGO- and rGO-based devices, carbon tape of length approximately 540 μm and width approximately 470 μm was used as the electrodes. Gas sensors based on the FGO or rGO on yarn were examined using a Keithley-4200 semiconductor parameter analyzer. NH_3 and NO_2 gases were introduced into the sensing chamber to analyze the resistance of the FGO- and rGO-based devices. The analytical gases used for the data collection were 0.5, 1.4, 2.7, 8.1, and 13.5 ppm NH_3 and 0.15, 0.5, 1, 3, and 5 ppm NO_2. FGO- and rGO-based sensors were placed at a 2 cm distance from the gas inlet, and all the gas sensing measurements were carried out at room temperature and under 25% relative humidity.

Conflicts of interest

There are no conflicts to declare.

Acknowledgements

This research was supported by a grant (2011-0031636) from the Center for Advanced Soft Electronics under the Global Frontier Research Program of the Ministry of Science, ICT and Future Planning, Korea. This research was also supported by Nano/Material Technology Development Program through the National Research Foundation of Korea (NRF) funded by the Ministry of Education, Science and Technology (NRF-2016M3A7B4900119).

Notes and references

1 S. Ehrmann, J. Jüngst, J. Goschnick and D. Everhard, *Sens. Actuators, B*, 2000, **65**, 247–249.
2 G. F. Fine, L. M. Cavanagh, A. Afonja and R. Binions, *Sensors*, 2010, **10**, 5469–5502.
3 M. Carotta, M. Ferroni, D. Gnani, V. Guidi, M. Merli, G. Martinelli, M. Casale and M. Notaro, *Sens. Actuators, B*, 1999, **58**, 310–317.
4 S. Ryabtsev, A. Shaposhnick, A. Lukin and E. Domashevskaya, *Sens. Actuators, B*, 1999, **59**, 26–29.
5 Q. Wan, Q. Li, Y. Chen, T.-H. Wang, X. He, J. Li and C. Lin, *Appl. Phys. Lett.*, 2004, **84**, 3654–3656.
6 E. Comini, G. Faglia, G. Sberveglieri, Z. Pan and Z. L. Wang, *Appl. Phys. Lett.*, 2002, **81**, 1869–1871.
7 E. Comini, *Anal. Chim. Acta*, 2006, **568**, 28–40.
8 F. Schedin, A. Geim, S. Morozov, E. Hill, P. Blake, M. Katsnelson and K. Novoselov, *Nat. Mater.*, 2007, **6**, 652–655.
9 J. D. Fowler, M. J. Allen, V. C. Tung, Y. Yang, R. B. Kaner and B. H. Weiller, *ACS Nano*, 2009, **3**, 301–306.
10 M. G. Chung, D. H. Kim, H. M. Lee, T. Kim, J. H. Choi, D. kyun Seo, J.-B. Yoo, S.-H. Hong, T. J. Kang and Y. H. Kim, *Sens. Actuators, B*, 2012, **166**, 172–176.
11 N. Hu, Z. Yang, Y. Wang, L. Zhang, Y. Wang, X. Huang, H. Wei, L. Wei and Y. Zhang, *Nanotechnology*, 2013, **25**, 025502.
12 Y. Dan, Y. Lu, N. J. Kybert, Z. Luo and A. C. Johnson, *Nano Lett.*, 2009, **9**, 1472–1475.
13 H. Song, L. Zhang, C. He, Y. Qu, Y. Tian and Y. Lv, *J. Mater. Chem.*, 2011, **21**, 5972–5977.
14 Z. Zhang, X. Zou, L. Xu, L. Liao, W. Liu, J. Ho, X. Xiao, C. Jiang and J. Li, *Nanoscale*, 2015, **7**, 10078–10084.
15 G. Singh, A. Choudhary, D. Haranath, A. G. Joshi, N. Singh, S. Singh and R. Pasricha, *Carbon*, 2012, **50**, 385–394.
16 P. A. Russo, N. Donato, S. G. Leonardi, S. Baek, D. E. Conte, G. Neri and N. Pinna, *Angew. Chem., Int. Ed.*, 2012, **51**, 11053–11057.

17 R. K. Paul, S. Badhulika, N. M. Saucedo and A. Mulchandani, *Anal. Chem.*, 2012, **84**, 8171–8178.
18 Y. Zhao, C. Hu, L. Song, L. Wang, G. Shi, L. Dai and L. Qu, *Energy Environ. Sci.*, 2014, **7**, 1913–1918.
19 G. Lu, L. E. Ocola and J. Chen, *Appl. Phys. Lett.*, 2009, **94**, 083111.
20 N. Hu, Y. Wang, J. Chai, R. Gao, Z. Yang, E. S.-W. Kong and Y. Zhang, *Sens. Actuators, B*, 2012, **163**, 107–114.
21 W. S. Hummers Jr and R. E. Offeman, *J. Am. Chem. Soc.*, 1958, **80**, 1339.
22 D. C. Marcano, D. V. Kosynkin, J. M. Berlin, A. Sinitskii, Z. Sun, A. Slesarev, L. B. Alemany, W. Lu and J. M. Tour, *ACS Nano*, 2010, **4**, 4806–4814.
23 S. Ji, B. K. Min, S. K. Kim, S. Myung, M. Kang, H.-S. Shin, W. Song, J. Heo, J. Lim and K.-S. An, *Appl. Surf. Sci.*, 2017, **419**, 252–258.
24 S. Some, Y. Xu, Y. Kim, Y. Yoon, H. Qin, A. Kulkarni, T. Kim and H. Lee, *Sci. Rep.*, 2013, **3**, 1868.
25 T. Yamashita and P. Hayes, *Appl. Surf. Sci.*, 2008, **254**, 2441–2449.
26 D. Yang, A. Velamakanni, G. Bozoklu, S. Park, M. Stoller, R. D. Piner, S. Stankovich, I. Jung, D. A. Field and C. A. Ventrice, *Carbon*, 2009, **47**, 145–152.
27 A. Kaniyoor and S. Ramaprabhu, *AIP Adv.*, 2012, **2**, 032183.
28 F. Yavari, Z. Chen, A. V. Thomas, W. Ren, H.-M. Cheng and N. Koratkar, *Sci. Rep.*, 2011, **1**, 166.
29 F. Yavari, E. Castillo, H. Gullapalli, P. M. Ajayan and N. Koratkar, *Appl. Phys. Lett.*, 2012, **100**, 203120.
30 O. Leenaerts, B. Partoens and F. Peeters, *Phys. Rev. B: Condens. Matter Mater. Phys.*, 2008, **77**, 125416.
31 S.-H. Kang, T.-H. Fang and Z.-H. Hong, *J. Phys. Chem. Solids*, 2013, **74**, 1783–1793.
32 Y. J. Yun, W. G. Hong, N.-J. Choi, B. H. Kim, Y. Jun and H.-K. Lee, *Sci. Rep.*, 2015, **5**, 10904.
33 Y. J. Yun, C. S. Ah, W. G. Hong, H. J. Kim, J. Shin and Y. Jun, *Nanoscale*, 2017, **9**, 11439–11445.